Magnetic focusing of cold atomic beam with a 2D array of current-carrying wires

Yang Liu (刘 泱), Min Yun (恽 旻), and Jianping Yin (印建平)

Key Laboratory for Optical and Magnetic Resonance Spectroscopy, Department of Physics, East China Normal University, Shanghai 200062

Received March 3, 2006

A new scheme to realize a two-dimensional (2D) array of magnetic micro-lenses for a cold atomic beam, formed by an array of square current-carrying wires, is proposed. We calculate the spatial distributions of the magnetic fields from the array of current-carrying wires and the magnetic focusing potential for cold rubidium atoms, and study the dynamic focusing processes of cold atoms passing through the magnetic micro-lens array and its focusing properties by using Monte-Carlo simulations and trajectory tracing method. The result shows that the proposed micro-lens array can be used to focus effectively a cold atomic beam, even to load ultracold atoms or a BEC sample into a 2D optical lattice formed by blue detuned hollow beams.

OCIS codes: 020.0020, 220.3620, 220.2560, 020.7490.

In atom optics, the focusing of cold atoms is one of the basic techniques to manipulate and control neutral atoms, in which focusing of a cold atomic beam is an important and popular candidate. The focusing of cold atoms relies on the interactions either of magnetic fields or of light fields with neutral atoms. For example, a red-detuned continuous wave laser was proposed to focus an atomic beam, which was first demonstrated by Bjorkholm *et al.*[1]. Later Balykin *et al.* used two counter-propagating laser beams to form an atom lens[2,3]. Subsequently, to reduce the spontaneous-emission aberrations, the application of a blue-detuned, hollow laser beam was suggested to focus a cold atomic beam[4,5]. More recently, the scheme of atom lens using standing-wave laser field has been developed and attracted more attention[6−10].

However, there is a challenge to avoid heating of the atoms during the focusing process. Although adiabatic focusing with a blue-detuned standing-wave light[9] and the artifice of "kicks"[10] was suggested later, the influence of photon scattering still exists. For this, Christensen *et al.*[11] first proposed a focusing scheme by using inhomogeneous magnetic field, which was demonstrated experimentally by Cornell *et al.*[12]. In recent years, various magnetic focusing schemes for cold atoms, such as using strong permanent magnets[13], or pulsed magnetic field[14−17] etc., have been proposed and demonstrated. Since it is difficult to alter the magnetic fields for permanent magnets, whereas the magnetic fields generated by current-carrying wires can be easily changed, both theoretical and experimental studies on the magnetic manipulations and controls of cold atoms using current-carrying wires have obtained fast development, and a new field as called "integrated atom optics" has being formed.

In this paper, we propose a novel and simple scheme to form a two-dimensional (2D) array of magnetic micro-lens for cold atomic beam using a spatially-varying magnetic field, which is generated by an array of square current-carrying wires. This scheme can produce a suitable magnetic field gradient to transversely compress a cold atomic beam. We also use Monte-Carlo simulations to study the dynamical focusing behavior of a cold ^{87}Rb atomic beam in the magnetic field of our micro-lens array scheme.

As shown in Fig. 1, the focusing scheme of a cold atomic beam is consisted of a series of straight and L-shaped current-carrying wires, which are fabricated on the surface of a substrate, forming a 3×3 array of square wire loop. In our scheme, all the wires on the XOY plane carry the same current I, and the size of each square wire is $a \times a$, the distance between adjacent wire loops is d, and the space between centers of adjacent wire loops is c. The unit cell of the array of the square wires is shown in Fig. 1(b). To realize the manipulation and control of the cold atomic beam along the Z direction, square holes ($b \times b$) at the center region of each square wire are excavated on the substrate.

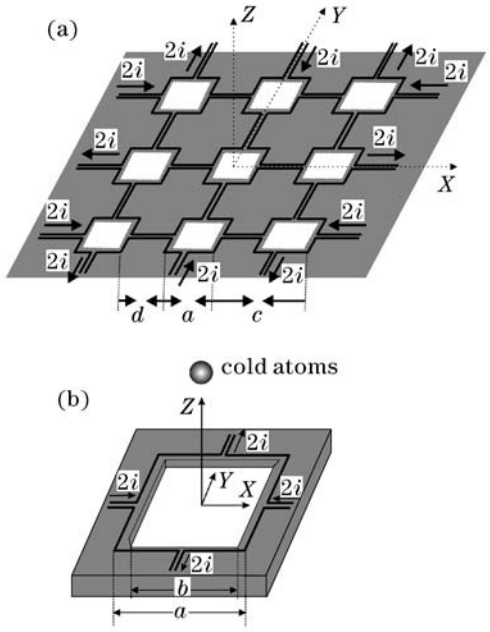

Fig. 1. (a) Schematic diagram of 2D 3×3 array of atomic lenses; (b) scheme of unit cell in our square-wire layout fabricated on a substrate with a square hole at each cell center.

According to the Ampere's circuit law, the spatial distribution of the magnetic field B in the plane of wires from our 3×3 array of square current-carrying wires can be calculated by

$$
\begin{aligned}
B = {} & \frac{\mu_0 I}{4\pi} \times \sum_{m=-1}^{1}\sum_{n=-1}^{1}(-1)^{m+n} \\
& \times \left\{ \int_0^{-a} \frac{-zi+(x+a-nc)k}{\left[(x+a-nc)^2+(y-y'-mc)^2+z^2\right]^{3/2}}\mathrm{d}y' + \int_{-a}^{0} \frac{-zj+(y+a-mc)k}{\left[(x-x'-nc)^2+(y+a-mc)^2+z^2\right]^{3/2}}\mathrm{d}x' \right. \\
& + \int_0^{-a} \frac{-zi+(x-a-nc)k}{\left[(x-a-nc)^2+(y-y'-mc)^2+z^2\right]^{3/2}}\mathrm{d}y' + \int_0^{a} \frac{zi-(x-a-nc)k}{\left[(x-a-nc)^2+(y-y'-mc)^2+z^2\right]^{3/2}}\mathrm{d}y' \\
& + \int_0^{a} \frac{zi-(x+a-nc)k}{\left[(x+a-nc)^2+(y-y'-mc)^2+z^2\right]^{3/2}}\mathrm{d}y' + \int_{-a}^{0} \frac{-zj+(y-a-mc)k}{\left[(x-x'-nc)^2+(y-a-mc)^2+z^2\right]^{3/2}}\mathrm{d}x' \\
& \left. + \int_a^{0} \frac{zj-(y-a-mc)k}{\left[(x-x'-nc)^2+(y-a-mc)^2+z^2\right]^{3/2}}\mathrm{d}x' + \int_a^{0} \frac{zj-(y+a-mc)k}{\left[(x-x'-nc)^2+(y+a-mc)^2+z^2\right]^{3/2}}\mathrm{d}x' \right\} \\
& + \sum_{m=-1}^{1}\sum_{n=-1}^{1}(-1)^{m+n}\times(-1)\times\frac{\mu_0 I}{2\pi}\times\frac{(-y+mc)\,k}{(-y+mc)^2+z^2} \\
& \times \left(\frac{a/2+x+d/2-nc}{\left[(a/2+x+d/2-nc)^2+(y-mc)^2+z^2\right]^{3/2}} - \frac{a/2+x-nc}{\left[(a/2+x-nc)^2+(y-mc)^2+z^2\right]^{3/2}} \right) \\
& + \sum_{m=-1}^{1}\sum_{n=-1}^{1}(-1)^{m+n}\times\frac{\mu_0 I}{2\pi}\times\frac{(-y+mc)\,k}{(-y+mc)^2+z^2} \\
& \times \left(\frac{a/2-x+d/2+nc}{\left[(a/2-x+d/2+nc)^2+(y-mc)^2+z^2\right]^{3/2}} - \frac{a/2-x+nc}{\left[(a/2-x+nc)^2+(y-mc)^2+z^2\right]^{3/2}} \right) \\
& + \sum_{m=-1}^{1}\sum_{n=-1}^{1}(-1)^{m+n}\times(-1)\times\frac{\mu_0 I}{2\pi}\times\frac{(x-nc)\,k}{(x-nc)^2+z^2} \\
& \times \left(\frac{-(a/2-y+mc)}{\left[(x-nc)^2+(a/2-y+mc)^2+z^2\right]^{3/2}} - \frac{a/2-y+d/2+mc}{\left[(x-nc)^2+(a/2-y+d/2+mc)^2+z^2\right]^{3/2}} \right) \\
& + \sum_{m=-1}^{1}\sum_{n=-1}^{1}(-1)^{m+n}\times\frac{\mu_0 I}{2\pi}\times\frac{(x-nc)\,k}{(x-nc)^2+z^2} \\
& \times \left(\frac{-(a/2+y-mc)}{\left[(x-nc)^2+(a/2+y-mc)^2+z^2\right]^{3/2}} - \frac{a/2+y+d/2-mc}{\left[(x-nc)^2+(a/2+y+d/2-mc)^2+z^2\right]^{3/2}} \right). \qquad (1)
\end{aligned}
$$

From Eq. (1), we can calculate the spatial distribution of the magnetic field $|B|$ of our array of square current-carrying wires, and then the corresponding magnetic potential for cold atom and its dipole gradient force can be calculated and analyzed (see Fig. 2). When a cold atom with a magnetic dipole moment $\overrightarrow{\mu}$ interacts with an inhomogeneous magnetic field, the magnetic dipole gradient force acting on a cold atom is given by

$$
\begin{aligned}
F_{\mathrm{mag}}(\vec{r}) &= -\nabla U_{\mathrm{dip}}(\vec{r}) = \nabla\left(\overrightarrow{\mu}\cdot\overrightarrow{B(\vec{r})}\right) \\
&= m_{\mathrm{F}} g_{\mathrm{F}} \mu_{\mathrm{B}} \nabla B(\vec{r}), \qquad (2)
\end{aligned}
$$

where m_{F} is the magnetic quantum number, g_{F} is the Lande G-factor, and μ_{B} is the Bohr magneton. We can see from Eq. (2) that when $\overrightarrow{\mu}\cdot\overrightarrow{B}<0$ (i.e., $\overrightarrow{\mu}\,/\!/\,-\overrightarrow{B(r)}$), the potential is repulsive, and the atoms in a weak-field-seeking state will be repelled to the minimum of the magnetic field by the dipole gradient force, which can be used to compressed transversely a cold atomic beam and then form an atom lens.

Figure 3 shows the contours of the magnetic field B from the wire layout with $a = 200$ μm, $b = 140$ μm, $c = 400$ μm, $d = 200$ μm, and $I = 50$ A. We can find that the

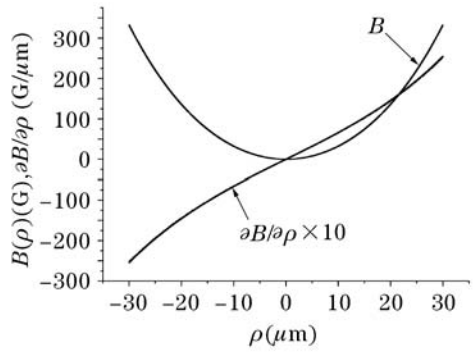

Fig. 2. Magnetic field distribution of each atomic lens and its gradient in wire plane for $I = 50$ A, $a = 200$ μm, $b = 200$ μm, $c = 400$ μm, and $d = 150$ μm. $\vec{\rho}$ is position vector in the diagonal direction ($y = x$).

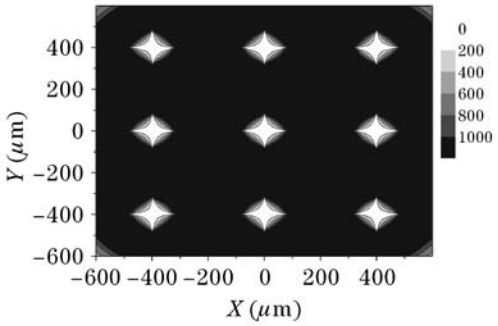

Fig. 3. Magnetic field contours of 2D array of square current-carrying wires on XOY plane for $a = 200$ μm, $b = 140$ μm, $c = 400$ μm, $d = 200$ μm, and $I = 50$ A. The interval between two adjacent contours is 200 G.

resulting magnetic field is a 2D quadrupole one, which is similar to one of atomic lens using permanent magnets[16] and a blue-detuned standing wave light[8]. Then, when a cold atomic beam passes through our array of square current-carrying wires on the substrate, it will be focused by the 2D quadrupole magnetic fields. So the proposed wire layout can be used to focus cold atoms or a cold atomic beam and form an array of atomic micro-lens.

To analyze the dynamic focusing processes of a cold rubidium atomic beam and its focusing properties, we perform a Monte-Carlo simulation and use a trajectory tracing method. In our scheme, a cold ^{87}Rb atomic beam with a number of $N = 6 \times 10^4$ is produced by using the technique of low-velocity intense source (LVIS) of atoms[18−21]. Cold ^{87}Rb atoms are first prepared in the $|F = 2, m_F = -2\rangle$ state, and then are pushed downwards by an imbalance of the radiation force. The longitudinal velocity distribution of the ^{87}Rb atomic beam can be tuned continuously by changing the intensity and frequency detuning of the forcing beam. Here we assume that the longitudinal velocity distribution of the ^{87}Rb beam is centered at 3 m/s with a full width half-maximum (FWHM) of 0.4 m/s, and the transverse temperature of the cold atomic beam is 40 μK. In our simulations, collision among cold atoms is ignored for convenience, and the classical atomic trajectory is simulated by employing an appropriate time step size of a microsecond. In the focusing process, we trace the trajectory of each atom in the atomic beam, and detect the atomic number in every z plane, so it is guaranteed that the focal plane

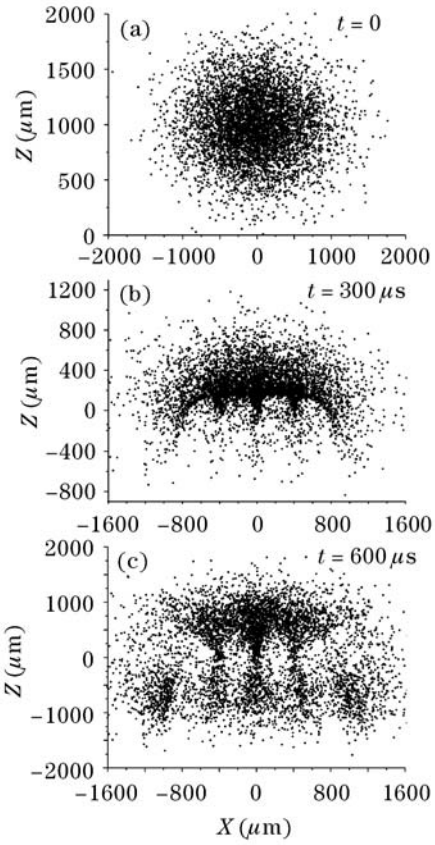

Fig. 4. Illustration of the focusing dynamic process and 2D distribution of cold atoms on the XOZ plane for $I = 50$ A.

is one of the planes with maximum atomic density below each wire loop. Figure 4 shows the dynamic focusing process of the cold ^{87}Rb atomic beam, and Fig. 5 gives 2D atomic distribution on the different Z planes at $t = 500$ μs as they pass through our wire layout. As shown in Fig. 5, the atomic beam is gradually focused and then defocused during the whole process, and the focal length f of each magnetic lens is 18 μm.

From the simple derivation[13], the focal length f of our magnetic lens can be expressed as

$$f = \frac{DE_{\rm kin}}{\mu_{\rm B}\beta L}, \tag{3}$$

where D and L are the aperture of the magnetic lens and the length of the effective magnetic field respectively, $E_{\rm kin}$ is the longitudinal kinetic energy of cold atoms, and $\beta = {\rm d}B/{\rm d}\rho$ is the mean transversal magnetic-field gradient. Here $\beta = 30$ T/cm in the effective focusing region, $D = 400$ μm, and $L = 500$ μm. According to these parameters and Eq. (3), we obtain $f \approx 18.7$ μm, which is in good agreement with our simulating result as given above.

Our square wire loop can be fabricated on a sapphire (or Al_2O_3 ceramic) substrate by using photolithography and electroplating techniques[22]. In 1998, the experimental result of Prentiss's group shows that an Au wire on a sapphire substrate can support the current of a few Amperes with a current density of $\sim 10^8$ A/cm^2 and a power dissipation of ~ 10 kW/cm^2 at liquid nitrogen (or helium) temperature in vacuum due to the heating

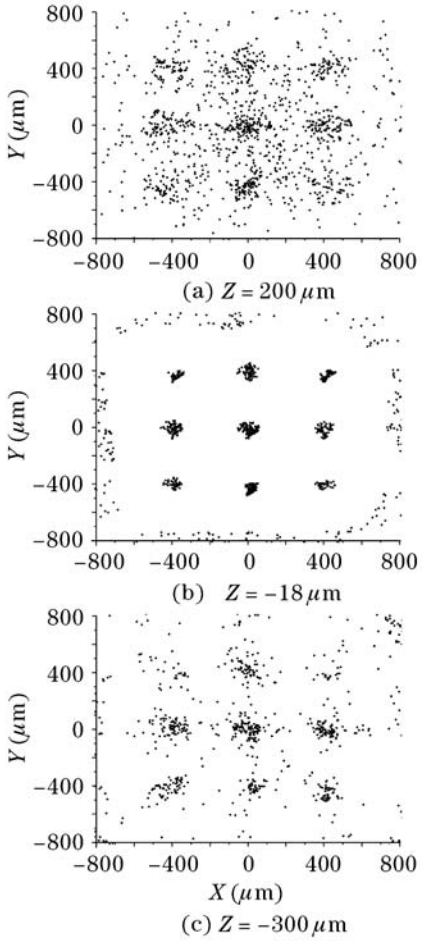

Fig. 5. Atomic distribution in three different XOY planes at $t = 500$ μs during the simulated focusing processes.

dissipation. For our magnetic micro-lens, when the width and the thickness of the wire as well as the current are chosen as $w = 40$ μm, $h = 30$ μm, and $I = 50$ A respectively, the corresponding current density I/wh is 4.165×10^6 A/cm^2, which is far lower than $\sim 10^8$ A/cm^2. So the cooling problem of our current-carrying wires can be resolved well by using liquid nitrogen even by use of cold cycle water.

In summary, we have proposed a novel scheme to focus a cold atomic beam based on the interaction of an atomic magnetic dipole moment of the focused atom with a magnetic field generated by a 2D array of square current-carrying wires. We have also calculated the contours of the resulting magnetic field and the transverse trapping potential and deflecting force for the ^{87}Rb atoms, and analyzed the dynamic focusing process and its focusing properties by using Monte-Carlo simulations and trajectory tracing method. Our study shows that the ^{87}Rb atomic beam can be strongly focused by our wire layout and the focal length of each magnetic micro-lens is 18.7 μm, which is consistent with our simulating result. So our scheme cannot only be used to focus cold atoms or cold atomic beam, and then to form a 2D array of atomic micro-lenses, but also have some important applications in atom optics and atomic lithography[23], such as the efficient loading of atoms into miniaturized traps and matter-wave guides[24−26], even to load ultracold atoms or a BEC into a 2D optical lattice formed by blue detuned hollow beams, and manufacture of atom-optical devices[27,28], etc..

This work was supported by the National Natural Science Foundation of China (No. 10174050, 10374029, and 10434060), the Shanghai Priority Academic Discipline, and the 211 Foundation of the Educational Ministry of China. J. Yin is the author to whom the correspondence should be addressed, his e-mail address is jpyin@phy.ecnu.edu.cn.

References

1. J. E. Bjorkholm, R. R. Freeman, A. Ashkin, and D. B. Pearson, Phys. Rev. Lett. **41,** 1361 (1978).
2. V. I. Balykin and V. S. Letokhov, Opt. Commun. **64,** 151 (1987).
3. V. I. Balykin, V. S. Letokhov, Yu. B. Ovchinnikov, and A. I. Sidorov, J. Mod. Opt. **35,** 17 (1988).
4. M. K. Olsen, T. Wong, S. M. Tan, and D. F. Walls, Phys. Rev. A **53,** 3358 (1996).
5. Lars Egil Helseth, Phys. Rev. A **66,** 053609 (2002).
6. G. Timp, R. E. Behringer, D. M. Tennant, and J. E. Cunningham, Phys. Rev. Lett. **69,** 1636 (1992).
7. J. J. McClelland, R. E. Scholten, E. C. Palm, and R. J. Celotta, Science **262,** 877 (1993).
8. L. Khaykovich and N. Davidson, Appl. Phys. B **70,** 683 (2000).
9. R. J. Celotta, R. Gupta, R. E. Scholten, and J. J. McClelland, J. Appl. Phys. **79,** 6079 (1996).
10. W. H. Oskay, D. A. Steck, and M. G. Raizen, Phys. Rev. Lett. **89,** 283001 (2002).
11. R. L. Christensen and D. R. Hamilton, Rev. Sci. Instrum. **30,** 356 (1959).
12. E. A. Cornell, C. Monroe, and C. E. Wieman, Phys. Rev. Lett. **67,** 2439 (1991).
13. W. G. Kaenders, F. Lison, I. Müller, A. Richter, R. Wynands, and D. Meschede, Phys. Rev. A **54,** 5067 (1996).
14. E. Maréchal, S. Guibal, J.-L. Bossennec, R. Barbé, J.-C. Keller, and O. Gorceix, Phys. Rev. A **59,** 4636 (1999).
15. T. Miossec, R. Barbe, J.-C. Keller, and O. Gorceix, Opt. Commun. **209,** 349 (2002).
16. M. J. Pritchard, A. S. Arnold, D. A. Smith, and I. G. Hughes, J. Phys. B **37,** 4435 (2004).
17. A. S. Arnold, M. J. Pritchard, D. A. Smith, and I. G. Hughes, New J. Phys. **8,** 53 (2006).
18. K. Dieckmann, R. J. C. Spreeuw, M. Weidemüller, and J. T. M. Walraven, Phys. Rev. A **58,** 3891 (1998).
19. Z. T. Lu, K. L. Corwin, M. J. Renn, M. H. Anderson, E. A. Cornell, and C. E. Wieman, Phys. Rev. Lett. **77,** 3331 (1996).
20. K. H. Kim, K. I. Lee, H. R. Noh, and W. Jhe, Phys. Rev. A **64,** 013402 (2001).
21. K. Kim, H.-R. Noh, Y.-H. Yeon, V. G. Minogin, and W. Jhe, Phys. Rev. A **65,** 055404 (2002).
22. M. Drndic, K. S. Johnson, J. H. Thywissen, M. Prentiss, and R. M. Westervelt, Appl. Phys. Lett. **72,** 2906 (1998).
23. D. Meschede and H. Metcalf, J. Phys. D **36,** 17 (2003).
24. D. Müller, D. Z. Anderson, R. J. Grow, P. D. D. Schwindt, and E. A. Cornell, Phys. Rev. Lett. **83,** 5194 (1999).
25. N. H. Dekker, C. S. Lee, V. Lorent, J. H. Thywissen, S. P. Smith, M. Drndic, R. M. Westervelt, and M. Prentiss, Phys. Rev. Lett. **84,** 1124 (2000).
26. M. Key, I. G. Hughes, W. Rooijakkers, B. E. Sauer, and E. A. Hinds, Phys. Rev. Lett. **84,** 1371 (2000).
27. J. Reichel, Appl. Phys. B **75,** 469 (2002).
28. E. A. Hinds and I. G. Hughes, J. Phys. D **32,** 119 (1999).